Femtosecond Neodymium-doped microstructure fiber laser

Mathias Moenster, Peter Glas, and Günter Steinmeyer

Max-Born-Institut für Nichtlineare Optik und Kurzzeitspektroskopie (MBI)
Max-Born-Str. 2a, 12489 Berlin, Germany
moenster@mbi-berlin.de

Rumen Iliew

Friedrich-Schiller-Universität Jena
Institut für Festkörpertheorie und Theoretische Optik
Max-Wien-Platz 1, 07743 Jena, Germany

Nikolay Lebedev and Reiner Wedell

Institut für angewandte Photonik e.V.
Rudower Chaussee 29/31, 12489 Berlin, Germany

Mario Bretschneider

Institute for Scientific Instruments GmbH
Rudower Chaussee 29/31, 12489 Berlin, Germany

Abstract: We demonstrate femtosecond operation of a Nd-doped microstructure fiber laser. The fiber provides gain and anomalous dispersion at the lasing wavelength of 1.06 μm and enables the construction of short and simple cavity designs. The laser is passively mode-locked by the combined action of a saturable absorber mirror, fiber nonlinearity, and dispersion and produces transform limited sub-400-fs pulses with a pulse energy as high as 100 pJ.

© 2005 Optical Society of America

OCIS codes: (140.3510) Lasers, fiber; (320.7090) Ultrafast lasers.

References and links

1. B. C. Collings, K. Bergman, S. T. Cundiff, S. Tsuda, J. N. Kutz, J. E. Cunningham, W. Y. Jan, M. Koch, and W. H. Knox, "Short Cavity Erbium/Ytterbium Fiber Lasers Mode-Locked with a Saturable Bragg Reflector," IEEE J. Sel. Top. Quantum Electron. **3**, 1065-75 (1997).
2. L. E. Nelson, D. J. Jones, K. Tamura, H. A. Haus, and E. P. Ippen, "Ultrashort-pulse fiber ring lasers," Appl. Phys. B **65**, 277-94 (1997).
3. M. Hofer, M. E. Fermann, F. Haberl, M. H. Ober, and A. J. Schmidt, "Mode locking with cross-phase and self-phase modulation," Opt. Lett. **16**, 502-4 (1991).
4. M. H. Ober, M. Hofer, U. Keller, and T. H. Chiu, "Self-starting diode-pumped femtosecond Nd fiber laser," Opt. Lett. **18**, 1532-4 (1993).
5. H. Lim, F. Ö. Ilday, and F. W. Wise, "Generation of 2-nJ pulses from a femtosecond ytterbium fiber laser," Opt. Lett. **28**, 660-662 (2003).
6. P. St. J. Russell, "Photonic Crystal Fibers," Science **299**, 358-62 (2003).
7. L. P. Shen, W. P. Huang, and S. S. Jian, "Design of Photonic Crystal Fibers for Dispersion-Related Applications," J. Lightwave Technol. **21**, 1644-51 (2003).
8. J. K. Ranka, R. S. Windeler, A. J. Stentz, "Visible Continuum generation in air-silica microstructure optical fibers with anomalous dispersion at 800 nm," Opt. Lett. **25**, 25-7 (2000).
9. H. Lim, F. Ö. Ilday, and F. W. Wise, "Femtosecond ytterbium fiber laser with photonic crystal fiber for dispersion control," Opt. Express **11**, 1497-2 (2002), http://www.opticsexpress.org/abstract.cfm?URI=OPEX-10-25-1497.
10. A. V. Avdokhin, S. V. Popov, and J. R. Taylor, "Totally fiber integrated, figure-of-eight, femtosecond source at 1065 nm," Opt. Express **11**, 265-9 (2003), http://www.opticsexpress.org/abstract.cfm?URI=OPEX-11-3-265.

11. K. Furusawa, T. M. Monro, P. Petropoulos, and D. J. Richardson, "Modelocked laser based on Ytterbium doped holey fibre," Electron. Lett. **37**, 560-1 (2001).

12. D. Mogilevtsev, T. A. Birks, P. St. J. Russell, "Group-velocity dispersion in photonic crystal fibers," Opt. Lett. **23**, 1662-4 (1998).

13. U. Keller, K. J. Weingarten, F. X. Kärtner, D. Kopf, B. Braun, I. D. Jung, R. Fluck, C. Hönninger, N. Matuschek, and J. Aus der Au, "Semiconductor Saturable Absorber Mirrors (SESAM's) for Femtosecond to Nanosecond Pulse Generation in Solid-State-Lasers," IEEE J. Sel. Top. Quantum Electron. **2**, 435-53 (1996).

14. M. Haiml, R. Grange, and U. Keller, "Optical characterization of semiconductor saturable absorbers," Appl. Phys. B **79**, 331-9 (2004).

15. M. Moenster, P. Glas, G. Steinmeyer, and R. Iliew, "Mode-locked Nd-doped microstructure fiber laser," Opt. Express **12**, 4523-7 (2004), http://www.opticsexpress.org/abstract.cfm?URI=OPEX-12-19-4523.

16. S. M. J. Kelly, "Characteristic sideband instability of periodically amplified average soliton," Electron. Lett. **28**, 806-7 (1992).

17. T. R. Schibli, E. R. Thoen, F. X. Kärtner, E. P. Ippen, "Suppression of Q-switched mode locking and break-up into multiple pulses by inverse saturable absorption," Appl. Phys. B **70**, 41-9 (2000).

18. C. Hönninger, R. Paschotta, F. Morier-Genoud, M. Moser, and U. Keller, "Q-switching stability limits of continous-wave passive mode locking," J. Opt. Soc. Am. B **16**, 46-56 (1999).

19. F. X. Kärtner and U. Keller, "Stabilization of solitonlike pulses with a slow saturable absorber," Opt. Lett. **20**, 16-8 (1995).

1. Introduction

Mode-locked fiber lasers are highly stable and cost-effective femtosecond light sources. Fiber lasers can be made very compact and are effectively shielded from environmental influences, which often makes them the preferred choice for a laser oscillator. However, the generation of femtosecond pulses in fiber lasers by passive mode-locking has only found widespread use at wavelengths of about 1.5 μm [1, 2], because soliton formation and dispersion compensation is only possible in this spectral region in standard optical fibers. In contrast, passive mode-locking in the Nd- or Yb-bands always requires extra-fiber dispersion compensation schemes [3–5]. Recently, microstructure fibers (MSFs) have greatly extended the range of soliton formation outside the erbium band down to the visible wavelength range [6]. While this potential for engineering dispersion properties [7] has readily been exploited in supercontinuum experiments [8], there are only few examples for the use of dispersion scaling possibilities offered by MSFs, both, for passive mode-locking, combining passive MSFs and active regular fiber sections [9, 10], and also for active mode-locking [11]. We now demonstrate femtosecond pulse generation, using only the tailored properties of the MSF and a saturable absorber mirror (SAM). All other mechanisms required for passive mode-locking, namely dispersion scaling, the optical nonlinearity, and the laser gain have been incorporated into one microstuctured optical fiber.

2. Experimental setup

Our MSF was fabricated from a phosphate glass with refractive index $n = 1.535$. Using a soft glass instead of silica facilitates the fiber drawing process at relatively low temperatures ($600 - 640°C$) and allowed for the fiber to be drawn in a single step from a preform. Moreover, higher doping concentrations can be realized using phosphate glasses, which is important for short gain fibers. Our fiber exhibits a hexagonal symmetry, with a doped core acting as the central defect, see Fig. 1(a). The inner 5.2 μm^2 of the core have been doped with 4500 ppm Nd_2O_3. From this value we calculate a pump absorption coefficient of ≈ 1.5 cm^{-1}. The air holes have a diameter $d = 0.9$ μm and a pitch $\Lambda = 1.72$ μm, see Fig. 1(a). Based on the measured geometry, a numerical simulation of the mode field [12] indicates that the fiber is single-mode at $\lambda = 1.06$ μm and has a mode area $A_{\text{eff,MSF}} \approx 4$ μm^2. The phosphate glass used has a higher nonlinearity than silica glasses with a nonlinear refractive index $n_2 = 6 \times 10^{-16}$ cm^2/W. Together with the small mode field area, this yields a fiber nonlinearity $\gamma = 0.09$ W^{-1}m^{-1}. The calculated group

velocity dispersion of the idealized geometry is $-17\,\mathrm{ps^2/km}$. Experimentally we found that the MSF is birefringent. Using spectral interferometry we measured values of $\beta_{2,\mathrm{slow}} = -16\,\mathrm{ps^2/km}$ for the slow axis and $\beta_{2,\mathrm{fast}} = -13\,\mathrm{ps^2/km}$ for the fast axis of the MSF. We inserted an $L = 56\,\mathrm{cm}$
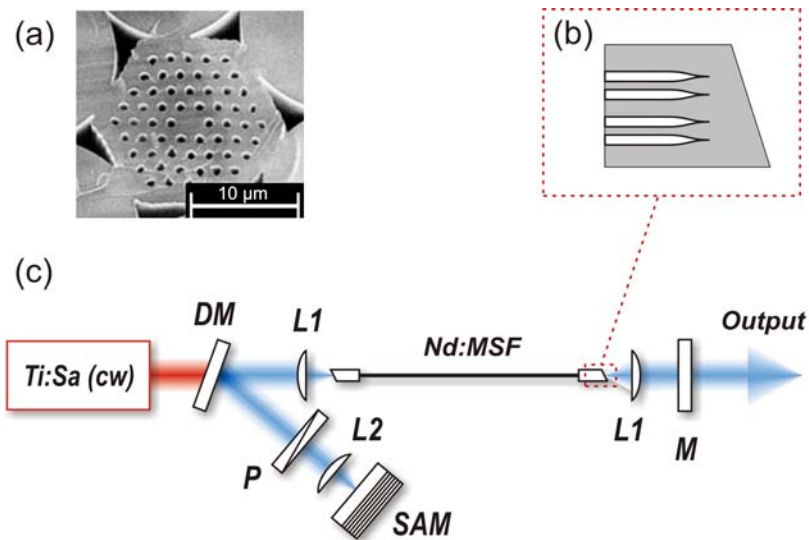

Fig. 1. (a) SEM micrograph of the fiber end face as cleaved. (b) Cross section of the two polished fiber end faces (schematically). (c) Laser setup. The blue beam indicates the path of the laser cavity whereas the red beam represents the pump radiation. DM: dichroic mirror ($T = 99\%$ at 810 nm, $R = 99\%$ at 1054 nm), L1, L2 : aspheric lenses ($f = 8\,\mathrm{mm}$, NA = 0.5), P: dichroic glass polarizer, M : output coupling mirror ($T = 30\%$ at 1054 nm), Ti:Sa: cw Ti:sapphire pump laser, Nd:MSF: Nd-doped microstructure fiber.

section of the doped MSF in the hybrid setup shown in Fig. 1(c), incorporating an additional $\approx 70\,\mathrm{cm}$ of air paths. We used a cw Ti:sapphire laser tuned to a wavelength of 810 nm as the pump source. About 100 mW of pump light is launched through a dichroic mirror into the MSF using an aspheric lens. The same type of aspheric lens is used on both sides of the fiber and for focusing on the SAM, which acts as one of the cavity end mirrors. The effective spot area on the SAM is estimated as $A_{\mathrm{eff,A}} \approx 3.5\,\mu\mathrm{m^2}$, i.e. nearly identical to the modal area in the fiber. The SAM displays a saturation fluence $F_{\mathrm{sat}} = 70\,\mu\mathrm{J/cm^2}$, a modulation depth $\Delta R = 14\%$, and a two-photon-absorption (TPA) fluence $F_2 \approx 1000 \times F_{\mathrm{sat}}$, with the SAM parameters as defined in Refs. [13] and [14], see Fig. 2(a). The recovery time was measured as $\tau_R = 10\,\mathrm{ps}$ [Fig. 2(b)]. On the opposite side of the cavity, we place a dielectric output coupling mirror. It should be noted that, given the relatively deep modulation of the SAM, we can afford a 30% output coupling.

To enable polarization selection, a thin polarizer is placed in front of the SAM. We find that the linear state of polarization as selected by the polarizer is preserved after passage through the fiber when used in a straight configuration. Furthermore it was possible to mode-lock the laser in various polarization angles, including angles which are offset from the polarization axes. A group velocity mismatch of $\approx 160\,\mathrm{fs}$ per roundtrip was found between the slow and fast axes by altering the polarizer angle while monitoring the repetition rate of the laser. From this measurement we deduce a fiber birefringence of $\Delta n = 3 \times 10^{-5}$. For the polarizer angle used in the following, we estimate an effective group velocity dispersion of $\beta_2 = -15\,\mathrm{ps^2/km}$. It is well known that Fresnel reflections from the fiber end faces can give rise to subcavity effects, preventing mode-locking of the laser. Angle cleaving or polishing is a common way to
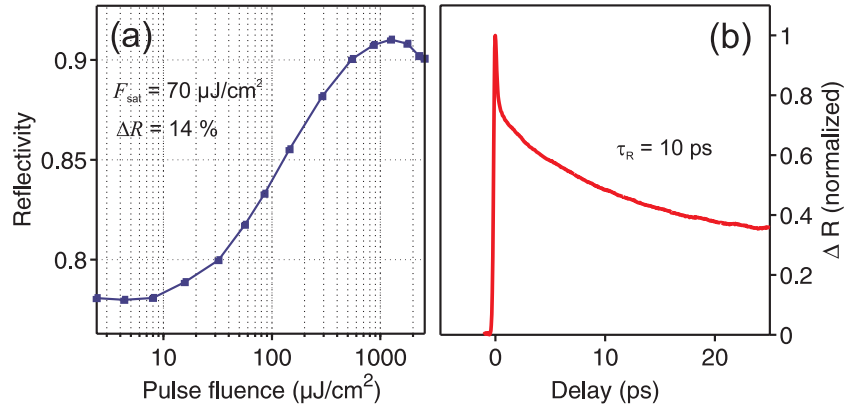
Fig. 2. (a) Measured SAM reflectivity vs. input pulse fluence. The measurement setup was similar to the one described in Ref. [14]. (b) Measured pump-probe response (normalized) of the SAM. The pulse source used for both measurements was a 180-fs passively mode-locked Nd:glass laser tuned to 1060 nm.

circumvent this problem. However, these standard techniques cannot be applied to MSFs since the mechanical stress damages the fragile microstructure. To overcome these difficulties we further improved the end face sealing technique described in Ref. [15]. We first sealed the MSF end faces using the electric arc of a fusion splicer. The fusion splicer delivers a well-defined amount of energy to the end faces in a short time, which allows for controlled collapsing of the air holes, forming an adiabatic transition region between bulk and microstructure, as shown in Fig. 1(b). The fiber is finally mounted in a ferrule and angle-polished at an angle of $12°$. We experimentally found that the coupling efficiency of the laser signal entering the MSF is actually increased by this procedure from 33% to 50%, which indicates a favorable effect of the adiabatic matching section to the overall losses in the cavity.

3. Results and discussion

Using the setup of Fig. 1(c), the laser shows self-starting passive mode-locking with pulse energies of 100 pJ at a repetition rate of 95 MHz, i.e. an output power of 9.5 mW. This yields an efficiency of about 10% relative to the launched power. Figure 3 depicts the measured intensity autocorrelation of our laser. The measured data show excellent agreement with a hyperbolic secant pulse of $\tau = 394$ fs duration (FWHM). Experimentally we found that the pulse duration increases to 440 fs when the intracavity power is reduced by 30%. Increasing the delay range of the autocorrelator to its maximum (see inset of Fig. 3) does not reveal any satellite pulses. Together with a measured satellite-free oscilloscope trace, we conclude that there is no multiple pulsing of the laser. The laser spectrum which is shown in Fig. 4(a) exhibits a width of 3.1 nm (FWHM), which is already a significant part of the 20 nm gain bandwidth of Nd-doped phosphate glasses. The spectrum also agrees very well with the assumption of a hyperbolic secant pulse profile. The resulting time-bandwidth product is 0.326, i.e., the pulse is transform limited.

The spectrum shows no indication of Kelly sidebands [16], as they often arise in soliton lasers. From the measured pulse duration we calculate the spectral position of the Kelly sidebands with respect to the spectral peak value as $\Delta\lambda \approx \pm 9.2$ nm. In fact, in some experiments we could see Kelly sidebands exactly at the computed positions far out in the spectral wings of the pulse. The practical absence of such features in Fig. 4(a) can therefore not be interpreted as an indication against soliton formation but is dictated by the laser parameters, in particular
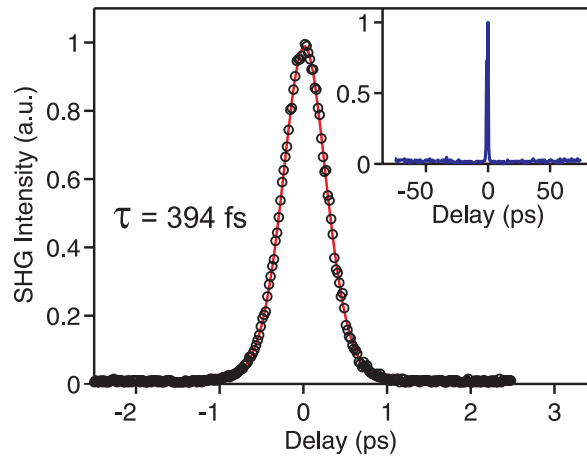
Fig. 3. Intensity autocorrelation. The measured data (black rings) have been fitted assuming a sech^2 pulse shape (red line). The inset shows the corresponding long-range autocorrelation.
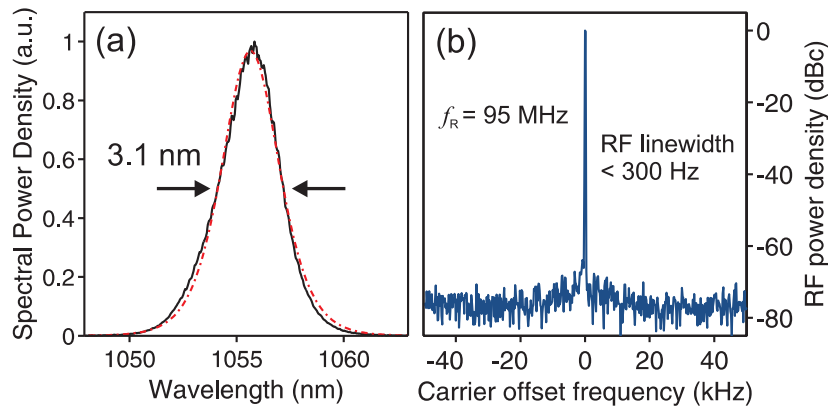

Fig. 4. (a) Optical spectrum of the mode-locked laser (resolution: 0.05 nm). The measured data (black line) has been fitted to the frequency representation of a sech^2 pulse spectrum (dash-dotted red line). (b) RF spectrum of the first intermode beat centered at $f_R \approx 95$ MHz (resolution bandwidth: 100 Hz).

the very short cavity length of our fiber laser. The latter prevents dispersive waves from being phasematched within three times the spectral half width. The resulting pulse fluence on the SAM is estimated as $F_P = 9500$ μJ/cm, which is about two orders of magnitude higher than the saturation fluence of the SAM. The measured SAM characteristics [Fig. 2.(a)] suggest that TPA processes can become relevant in this regime [17]. However, as shorter pulses (180 fs) were used for the characterization of the SAM than are present in our laser, TPA is expected to set in at higher fluences in our cavity.

To convince ourselves of the absence of Q-switched mode-locking, we measured the RF spectrum of the intermode beat of the mode-locked laser, see Fig. 4(b). We measure an RF linewidth of less than 300 Hz. Q-switching sidebands are at least ≈ 70 dB below the carrier, which is an extremely good value for a Nd-doped laser material. The key laser parameters that ensure stability against Q-switched mode-locking are the small mode area of the MSF and the

equally small spot size on the SAM. That Q-switched mode-locking is not an issue in our laser can be confirmed by the stability criterion of Hönninger *et al.* [18]. In its simplest form, this criterion requires that the pulse energy be larger than the geometric average of the saturation energies of gain and saturable absorption weighted with ΔR, i.e., $E_p > (E_{\text{sat,MSF}} E_{\text{sat,A}} \Delta R)^{1/2}$. Accounting for soliton filtering, an additional term further increases the left-hand side of the inequality. We find that the inequality is met for our laser with or without accounting for soliton filtering. This explains the practical absence of Q-switching artifacts in the RF spectrum.

It is quite obvious that the observed femtosecond pulse durations cannot be explained by saturable absorber mode-locking alone, other than in our previous experiments [15] where pulse durations closely followed the relaxation time constant of the SAM. The autocorrelation measurements and spectra are suggestive for a dominant role of solitons as the pulse shaping mechanism. However, for the measured values of dispersion and fiber nonlinearity, we compute a soliton area $E_s \tau_s = 2\beta_2/\gamma \approx 3 \times 10^{-25}$ Js, which is about two orders of magnitude below the measured product of pulse energy E_s and soliton duration $\tau_s = 0.56\tau$, which yields $E_s \tau_s = 7.5 \times 10^{-23}$ Js. In other words, our laser supports much higher pulse energies than compatible with a pure fundamental soliton mode-locking scenario. This gross deviation from the area theorem was also observed by Collings *et al.* for the case of an erbium fiber laser that was mode-locked by a saturable Bragg reflector [1]. One possible explanation for this discrepancy could be the on-set of pulse shaping from the fast absorber time constant, which is ruled by intraband relaxation effects [1, 13]. It should be noted, however, that the fast component in Fig. 2(b) is rather weak, amounting to only about one fifth of the total response amplitude. Alternatively, the femtosecond pulse duration may be explainable by the combined action of slow saturable absorption, self-phase modulation and dispersion. This behavior would be similar to soliton mode-locking of passively mode-locked solid-state bulk lasers [19]. Such solid-state laser cavities consist of discrete sections that either deliver dispersion or nonlinearity, which gives rise to quasi-solitonic behavior. It has to be pointed out that stable pulses form under the combined action of the SAM, dispersion, and self-phase modulation. The strong stabilizing action of the SAM may therefore allow higher pulse energies of the quasi-solitons than pure fiber cavities. One necessary criterion for soliton mode-locking is that the soliton period z_0 be long compared to the cavity length. This is typically accounted for by the requirement that the soliton phase per roundtrip $\phi_0 = \pi L/(2z_0) = L|\beta_2|/\tau_s^2 \approx 0.17$ be small compared to 0.1. Of course, this condition is less stringent for a laser with continuous nonlinearity and dispersion. On the other hand, however, the rather strong round trip action of the SAM and the stabilizing effect of gain filtering can probably not be considered perturbational anymore. Keeping this in mind, we estimate a minimum stable pulse width of about 200 fs (FWHM) within the framework of Ref. [19] when we use the measured roundtrip gain $g = 2$. This means that soliton mode-locking incorporating the action of a slow saturable absorber appears well compatible with our experimental findings, including the observed sech^2 pulse shape. At the current stage of the experiments, we can, however, not rule out a fast contribution from the SAM response as partially responsible for the observed femtosecond pulse duration.

4. Conclusion

To the best of our knowledge, we have, for the first time, directly exploited the dispersion scaling potential of MSFs to synthesize a gain medium with suitable dispersion properties for passively mode-locked operation. This was demonstrated with the generation of 400-fs pulses, using nothing but an additional SAM in the laser cavity. This allows for a very simple and compact architecture, making relatively high repetition rates for a fiber laser possible. Yet, with this first demonstration, the capacities for a compact, integrated setup have certainly not been fully exploited. Using ytterbium as the gain medium may allow for further shortening of the

fiber; butt-coupling of the SAM may contribute to a further increase of the repetition rate. With its potential for short fiber cavities, our laser appears as an interesting step towards a more bulk-like fiber laser. More importantly, however, our passively mode-locked MSF laser opens up a perspective for a compact femtosecond fiber laser working in the one-micron range, which is a promising source, e.g., for seeding amplifiers or metrology applications.

Acknowledgements